Exp. Anim. 66(4), 293–302, 2017

—Original—

Nitric oxide is critical for avoiding hepatic lipid overloading via IL-6 induction during liver regeneration after partial hepatectomy in mice

Yue YU[1)], Miho TAMAI[1–3)], and Yoh-ichi TAGAWA[1,2)]

[1)]*Department of Biomolecular Engineering, Graduate School of Bioscience and Biotechnology, Tokyo Institute of Technology, 4259 B51, Nagatsuta-cho, Midori-ku, Yokohama, Kanagawa 226-8501, Japan*
[2)]*School of Life Science and Technology, Tokyo Institute of Technology, 4259 B51, Nagatsuta-cho, Midori-ku, Yokohama, Kanagawa 226-8501, Japan*
[3)]*Course of Oral Medical Science, Graduate School of Dental Medicine, Hokkaido University, Kita 13-jo, Nishi 7-chome, Kita-ku, Sapporo, Hokkaido 060-8586, Japan*

Abstract: Nitric oxide (NO), generated from L-arginine by three different isoforms of nitric oxide synthase (NOS), is a pleiotropic factor to regulate physiological functions in almost every organ and tissue. Each knockout mouse of iNOS or eNOS has been used to suggest that NO has a crucial role in liver regeneration after partial hepatectomy (PH), for NO may inhibit caspase 3 activity and is required for EGFR signaling. In previous reports, defective mitochondrial β-oxidation was observed in eNOS KO mice, and hepatic steatosis was often correlated to deficient liver regeneration, so we focused on metabolic perspective and hypothesized that NO depletion in PH mice would affect hepatocytic lipolysis and impair hepatocytes proliferation. We inhibited all NOS isoforms by administrating L-N^{G}-nitroarginine methyl ester (L-NAME) to PH mice, and hepatocyte DNA synthesis was severely inhibited at 40–44 h post PH in L-NAME (+) group. IL-6 was robustly secreted into circulating blood in L-NAME (−) group, but not in L-NAME (+) group. Down-regulation of carnitine palmytoyltransferase 1A, massive lipid accumulation and elevated endoplasmic reticulum (ER) stress relative genes expression level were observed in L-NAME (+) group mouse liver. The expression level of C/EBP homologous protein, a mediator of ER stress induced apoptosis, significantly increased in L-NAME (+) group. Our findings suggest the lack of NO affected IL-6 induction and hepatocyte lipolysis after PH, consequently leading to excessive hepatic lipid accumulation, elevated ER stress and impaired hepatocyte proliferation.

Key words: ER stress, hepatic lipid, hepatocyte proliferation, nitric oxide

Introduction

Liver resection and transplantation are the most curative treatment for primary and secondary liver tumors [2, 21]. As a solution to the lack of the organ donors, partial liver donation from a living donor is feasible due to strong regenerative potential of liver. This phenomenon of liver regeneration has evolved to protect organisms from natural liver loss, which could be caused by food toxins or trauma. Investigations about liver regeneration have taken place in past decades to reveal its mechanism, however that is not fully understood [5, 15, 22, 33]. The mostly used experimental model to study liver regeneration is 68% partial hepatectomy (PH) on

(Received 8 February 2017 / Accepted 9 April 2017 / Published online in J-STAGE 18 May 2017)
Address corresponding: Y. Tagawa, Department of Biomolecular Engineering, Graduate School of Bioscience and Biotechnology, Tokyo Institute of Technology, 4259 B51, Nagatsuta-cho, Midori-ku, Yokohama, Kanagawa 226-8501, Japan
Supplementary Figures: refer to J-STAGE: https://www.jstage.jst.go.jp/browse/expanim

mouse or rat, neatly removing 2 out of 5 distinctly formed liver lobes [9, 13]. Mature hepatocytes, previously staying quiescent in G0 phase, can proliferate to restore liver mass while performing all their essential functions. This process is inducted by a redundant signaling network composed of mitogenic cytokines, growth factors, and metabolic factors.

Nitric oxide (NO) is a multifunctional signaling molecule involved in neural transmission, vessel validation, and immune response. It is synthesized by three isoforms of nitric oxide synthase (NOS) [18, 37, 38]. Constitutive endothelial NOS (eNOS) is expressed in liver to regulate hepatic perfusion, inducible NOS (iNOS) is expressed in almost every type of hepatic cells under certain stimulus, neuronal NOS (nNOS) is believed to be absent in liver for its lack of neural network. As a rapidly diffusible gaseous molecule, physiological functions of NO vary largely based on concentration, timing, and location. Its contradictory roles under different physiological and pathological conditions have been reported continuously in recent years. The function of NO in liver regeneration has been studied by transgenic mouse models. Mei *et al.* reported that eNOS is required for epidermal growth factor receptor (EGFR)-mediated cell-cycle progression after hepatectomy [20]. Rai *et al.* reported an increased hepatocyte apoptosis and excessive lipid accumulation of hepatocytes in iNOS KO mice after hepatectomy [26]. Because that excessive hepatic lipid accumulation often correlates with deficient liver regeneration after PH [11, 29, 35], and several evidence suggested NO has a function to regulate lipid metabolism [8,16], we hypothesized that NO depletion in PH mice would affect fatty acid β-oxidation in hepatocyte, and excessive lipid accumulation in hepatocyte would impair its proliferation. Here, we inhibited all NOS isoforms by administrating a NOS inhibitor L-N^G-nitroarginine methyl ester (L-NAME) after hepatectomy. Using this systemic NO depletion model, we investigated functions of NO in liver regeneration in a metabolic perspective.

Materials and Methods

Animal experiments

BALB/cA mice were purchased from CLEA Japan, Inc. Male mice (6–10 weeks) were subjected to partial hepatectomy (PH) under adequate anesthesia via isoflurane (Abbott, Tokyo, Japan) inhalation, according to the original method of two third PH described by Higgins and Anderson [13] and a modified one on mouse model [9]. Left upper lobe, right upper lobe and left lower lobe were ligated and removed, which equaled 68% of mouse liver weight [9]. The surgery was performed during fixed period from 12:00 to 15:00.

IL-6 KO mice were originally generated by Kopf *et al.* [17]. The second exon of the IL-6 gene was disrupted by a *neo*^{r} cassette insertion. The original 129 × C57BL/6 IL-6 KO mice were backcrossed to BALB/cA mice in our lab. The experiments were conducted according to institutional and governmental guidelines for recombinant DNA experiments.

After hepatectomy, L-N^G-nitroarginine methyl ester (L-NAME) (Dojindo, Kumamoto, Japan) was administrated by intravenous injection, 100 mg/kg of body weight. To quantify hepatocyte proliferation, 5-bromo-2'-deoxyuridine (BrdU, Sigma-Aldrich, MO, USA) was administrated to PH mice 1 h before dissection and sampling, by intraperitoneal injection, 50 mg/kg of body weight.

All the mice were housed in a pathogen-free animal facility maintained at 25°C, illuminated by 12:12-h light-dark cycles, and provided with standard rodent chow and water *ad libitum*. The study protocols were approved by the Animal Experimentation Committees of Tokyo Institute of Technology.

Measurement of serum nitrite and β-hydroxybutyrate

Collected by cardiocentesis or retro orbital puncture, PH mouse blood was centrifuged (4°C, 3,000 rpm, 10 min) and serum was deproteinized using 30,000 MWCO (for nitrite assay) or 10,000 MWCO (for β-hydroxybutyrate assay) filter membrane (Sartorius, Göttingen, Germany). Serum nitrite concentration was measured with Griess Reaction System (Promega, WI, USA) and β-hydroxybutyrate was measured with β-hydroxybutyrate assay kit (Sigma-Aldrich, MO, USA).

Histological analysis

Right lower lobe in the remnant liver of PH mouse was fixed in Mildform®10N (Wako, Osaka, Japan). For immunohistostaining and hematoxylin/eosin (HE) staining, the fixed liver tissue was embedded in paraffin, and sliced in 4 μm sections (Bozo Research Center, Tokyo, Japan). HE staining was performed by Bozo Research Center, Tokyo, Japan. The sections were deparaffinized in xylene and rehydrated through graded alcohols to Milli-Q water, then microwaved till boiling in 10 mmol/l

citrate solution (pH 6.0). After natural cooling and 3 times wash with Tris-buffered saline (TBS) (pH 7.6), the section slides were incubated in 2 mol/l HCl, 37°C, 30 min, washed in TBS and incubated in Blocking One (Nacalai Tesque, Kyoto, Japan), room temperature, 30 min. Subsequently the slides were incubated in anti-BrdU antibody (ab6326, abcam, Cambridge, UK), 1:200, 4°C, 48 h, and goat anti-rat IgG conjugated with Alexa Fluor 594 (Invitrogen, CA, USA), 1:1,000, room temperature, 2 h.

To detect triglyceride content in hepatocytes, the fixed liver tissue was dipped in 15% and then 30% sucrose solution in phosphate buffered saline (PBS) for cryoprotection. After the liver tissue was embedded and frozen in O.C.T. compound (Sakura Finetek, CA, USA), 12 μm frozen sections were made by cryostat sectioning. 2.5 g Oil Red O (ORO, Sigma-Aldrich, MO, USA) was dissolved in 400 ml isopropyl alcohol as stock solution. ORO stock solution and Milli-Q water was 3:2 mixed as the working solution, then it is filtered and added on frozen sections for 5 min. Finally the sections were rinsed in tap water and mounted in EcoMount (Biocare Medical, CA, USA).

Measurement of plasma IL-6 activity

PH mouse blood was collected by cardiocentesis with heparin coated syringes and disposable needles. Plasma was separated by centrifugation (4°C, 3,000 rpm, 10 min), and sterilized by filtration with Millex 0.22 μm Filter Unit (Merck Millipore, MA, USA). After rapidly frozen with liquid nitrogen, plasma samples were stored in −80°C freezers, and later thawed by centrifugation (4°C, 10,000 rpm, 10 min) before added into assay culture wells.

IL-6 protein activity could be measured by a bio-assay using IL-6-dependently-proliferative hybridoma cell line (7TD1 cell) culture, which is described before [24, 30]. For regular cell culture, 7TD1 cell suspension culture was plated at a density of 2.0×10^4 cells/ml and incubated with 25 unit/ml recombinant murine IL-6 (Peprotech, NJ, USA), in RPMI1640 (Gibco, MA, USA) supplemented with 5% FBS (Gibco, MA, USA) and 25 μmol/l 2-Mercaptoethanol (Sigma-Aldrich, MO, USA).

For plasma IL-6 activity assay, 7TD1 cells were plated at a density of 2.0×10^4 cells/ml in flat-bottom 96 well plates, with 5% mouse plasma, or with serially diluted IL-6 solutions in culture media. Cell growth was assessed after 3 days of incubation by colorimetric test with Cell Counting Reagent SF (Nacalai Tesque, Kyoto, Japan), in a good measurement precision (Supplementary Fig.1).

Measurement of total lipid content

Total lipid was extracted by the classical Folch method [6]. Liver tissue (~200 mg) was homogenized in chloroform/methanol solution (v/v=2:1), and shook in room temperature for 6 h. After collecting the supernatant after centrifugation, 0.9% NaCl solution (w/w) was used to wash the liquid phase. Finally the liquid phase, mainly composed of chloroform and dissolved liver total lipid, was evaporated by a vacuum concentrator, the total lipid mass was measured by an analytical balance.

RNA isolation and real-time PCR

Total RNA was isolated using the acid guanidinium-phenol-chloroform method according to a standard protocol described before [31]. First-strand cDNA was prepared from the extracted total RNA in a reverse-transcriptase reaction, using the SuperScript II Reverse Transcriptase kit and oligo (dT) primer (Invitrogen, CA, USA) according to the instruction from manufacturer. The cDNA from mRNA of the genes of interest were amplified with a set of specific primers described in Table 1. Quantitative real-time RT-PCR was performed on StepOnePlus™ real-time PCR system (Applied Biosystems, CA, USA), using SYBR® Green Master Mix (Applied Biosystems, CA, USA).

Statistical analysis

The data were compared with one-way analysis of variance followed by Student's *t* test. A value of $P<0.05$ was considered statistically significant. All values are expressed as the mean ± SD.

Results

NO was transiently produced during liver regeneration after 68% PH and liver regeneration was disturbed by systemic inhibition of NOSs

BALB/cA male mice were operated 68% PH under anesthesia. After hepatectomy, generally the mice regained their liver mass within 7 days. To elucidate the relationship between NO and liver regeneration after hepatectomy, L-NAME (100 mg/kg-body weight), an effective inhibitor to all 3 isoforms of NOS, was administrated to BALB/c male mice at 3 h post PH (PH 3 h),

Table 1. Real-time PCR primer sequences

Gene name	Forward (5' to 3')	Reverse (5' to 3')
Hypoxanthine-guanine phosphoribosyltransferase (*Hprt*)	GTCAACGGGGGACATAAAAG	GCTTAACCAGGGAAAGCAAAG
Carnitine palmitoyltransferase 1A (*Cpt1a*)	AACAGCAAGATAGGCATAAACGC	CCATGACATACTCCCACAGATGG
Liver-type fatty acid binding protein (*LFabp*)	GAGGAGTGCGAACTGGAGACC	AGTTCAGTCACGGACTTTATGCC
Fatty acid transport protein 2 (*Fatp2*)	TGTCATCTATACCACAATGCCCC	TTGTATTTCCTGCAGTCGTCCC
Binding immunoglobulin protein (*Bip*)	TGGTATTGAAACTGTGGGAGGAG	GGTCGTTCACCTTCATAGACCTT
Inositol requiring enzyme 1α (*Ire1a*)	GAGGCAAGAACAACGAAGGC	AGGCCTGAACCAATTCTGGG
Activating transcription factor 6 (*Atf6*)	ATTCTCAGCTGATGGCTGTCC	AAACGTATCTCCCCTCCTGC
PKR-like ER kinase (*Perk*)	AGTCCCTGCTCGAATCTTCC	CTATCCCATCGGCGACATCC
Spliced form of X-box binding protein 1 (*sXbp1*)	AAAGAAAGCCCGGATGAGCG	CTGGTTCTCAACCACAAGGC
C/EBP homologous protein (*Chop*)	CGACAGAGCCAGAATAACAGC	CACCGTCTCCAAGGTGAAAGG

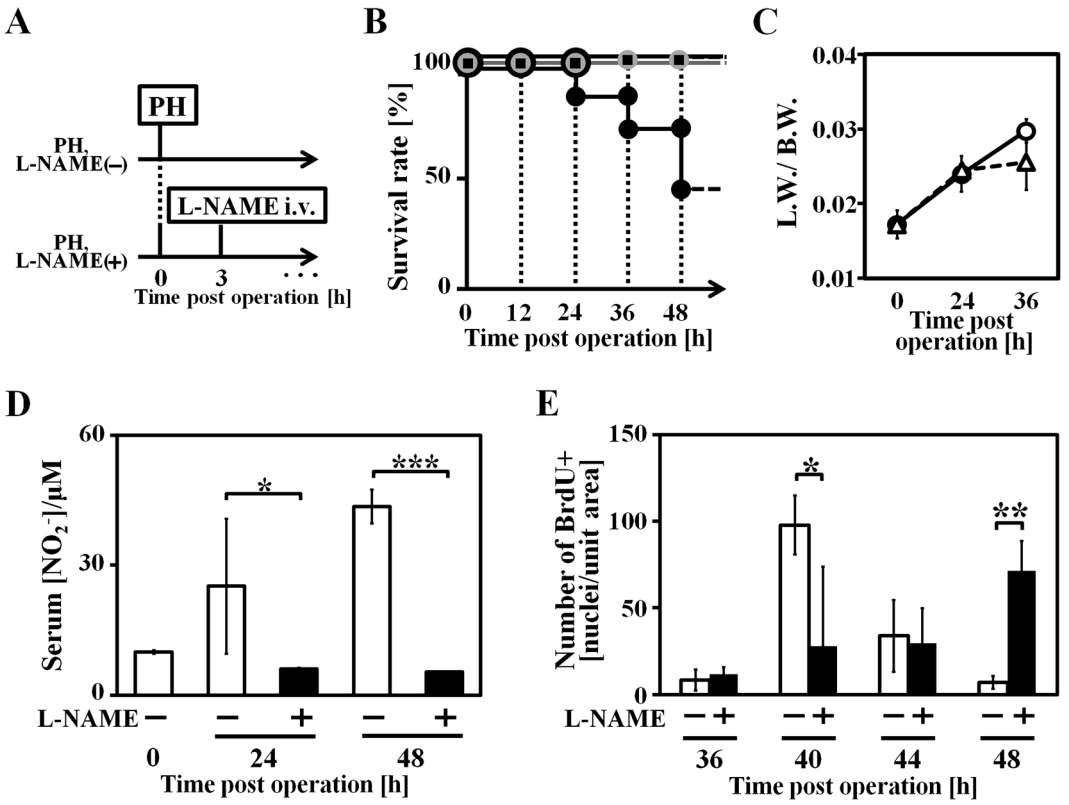

Fig. 1. Systemic NO depletion of PH mice by L-NAME administration. A: Animal experiment scheme, L-NAME was administrated intravenously 3 h after hepatectomy (PH 3 h), 100 mg/kg b.w. B: Survival rate of each groups after PH (black square dot: PH mice without L-NAME administration, L-NAME (−) group, n=20; grey round dot: L-NAME administrated mice without PH, n=5; black round dot: PH mice with L-NAME administration, L-NAME (+) group, n=24). C: Liver weight to body weight ratio (round dot: L-NAME (−) group; tri-angle dot: L-NAME (+) group), n=3. Liver weight data from both groups were calculated to exclude total lipid content (data shown in Fig. 2B). D: serum nitrite concentration, n=3. E: Quantification of BrdU positive hepatocytes per unit area, n=3–5. Data are represented as mean ± SD. * P<0.05, ** P<0.01 and *** P<0.005.

inhibiting NO production in a systemic scale (Fig. 1A).

Comparing to approximately 100% survival rate in L-NAME (−) group, L-NAME (+) group survival rate dropped to 41% in PH 48 h (Fig. 1B). Despite an obvious tendency to decrease in liver to body weight ratio of L-NAME (+) group, the data revealed no significance up to PH 36 h (Fig. 1C). To confirm successful NOS inhibition during liver regeneration, serum samples were

collected and centrifuged with molecular weight cut-off ultrafiltration membrane for deproteination, and serum nitrite level was measured as a scale of physiological NO production level. NO production level in L-NAME (+) group mice did not rise in the same manner with L-NAME (−) group mice at PH 24 h and 48 h (Fig. 1D).

L-NAME administration inhibited cell-cycle re-entry of hepatocyte and IL-6 secretion

The quantification of PH mice hepatocyte cell-cycle re-entry was determined by hepatocyte BrdU incorporation level. BrdU was administrated to PH mice 1 h before sacrifice, and hepatocytes incorporated BrdU was detected by immunohistostaining (Fig. 1E, supplementary Fig. 2). BrdU positive hepatocytes emerged abundantly around PH 40–44 h in L-NAME (−) group, but such hepatocytes were barely existing in L-NAME (+) group before PH 48 h. 40% L-NAME (+) group mice survived at PH 48 h (Fig. 1B), and their BrdU incorporation level of hepatocytes rose, revealing a delayed liver regeneration. Therefore, hepatocyte proliferation is severely impaired in L-NAME (+) group, and the reason of low survival rate before PH 48 h in L-NAME (+) group, could be ascribed to deficient liver regeneration.

Because IL-6-gp130-STAT3 pathway is fundamentally required to initiate liver regeneration, IL-6 activity level of mouse plasma from L-NAME (+) group, L-NAME (−) group, and also IL-6 KO group was quantified. After hepatectomy, IL-6 activity level in L-NAME (−) group increased robustly at PH 24 h, but could not be detected in L-NAME (+) group and IL-6 KO group mice at PH 0 h and PH 24 h (Table 2).

Table 2. Plasma IL-6 activity assay of L-NAME (−), L-NAME (+) and IL-6 KO group mice

$\log_{10}$ ([plasma IL-6]/(unit/ml))		
	Time post operation (h)	
	0	24
L-NAME (−)	N.D.	2.36 ± 1.11
L-NAME (+)	–	N.D.
IL-6 KO	N.D.	N.D.

Excessive lipid accumulation was observed in remnant liver of L-NAME (+) group after partial hepatectomy

Excessive lipid accumulation can be observed in livers of both L-NAME (−) and L-NAME (+) group at PH 24 h, from an obviously whitened color of liver and HE stained liver sections (Figs. 2A and B). Lipid drops could be detected by ORO staining, and compared to L-NAME (−) group, hepatic lipid accumulation in L-NAME (+) was slightly more severe after hepatectomy (Fig. 2C). We used Folch method to quantify total lipid (TL) content in liver samples (Fig. 2D), and TL content in L-NAME (+) group liver was significantly higher than L-NAME (−) group.

Gene expression of important enzyme and transporters which are related to hepatic lipolysis, was analyzed by real-time PCR (Fig. 3A). β-oxidation speed-control step enzyme carnitine palmitoyltransferase 1A (*Cpt1a*) expression at PH 24 h in L-NAME (+) group was remarkably down-regulated compared to L-NAME (−) group. Fatty acid transporters liver-type fatty acid binding protein (*LFabp*) and fatty acid transport protein 2 (*Fatp2*) expressions were comparable in both groups at each time point.

β-hydroxybutyrate is a final product of ketogenesis and an indicator of the degree of fatty acid β-oxidation, its plasma concentration was measured by a coupled enzyme reaction (Fig. 3B). In L-NAME (−) group β-hydroxybutyrate level was comparable between PH 0 h and 24 h, however in L-NAME (+) group, serum β-hydroxybutyrate level rose significantly in PH 24 h.

Endoplasmic reticulum (ER) stress was increased in remnant liver after partial hepatectomy by L-NAME administration

Because intracellular lipid accumulation could cause elevated ER stress, we compared ER stress relative gene mRNA levels in L-NAME (−) and L-NAME (+) group mice liver by real-time PCR (Fig. 4). Binding immunoglobulin protein (*Bip*) is the adjustor of ER stress and regulator of unfolded protein response (UPR), its expression increased in both groups up to PH 36 h. Among 3 ER stress sensors, inositol requiring enzyme 1α (*Ire1a*) and activating transcription factor 6 (*Atf6*) expression increased first at PH 24 h, then decreased at PH 36 h as *Bip* expression increased. In L-NAME (+) group, another ER stress sensor PKR-like ER kinase (*Perk*) expression increased significantly in PH 24 h compared to L-NAME (−) group, and C/EBP homologous protein (*Chop*), downstream of *Perk* and a mediator of ER stress induced apoptosis, significantly increased in PH 24 h.

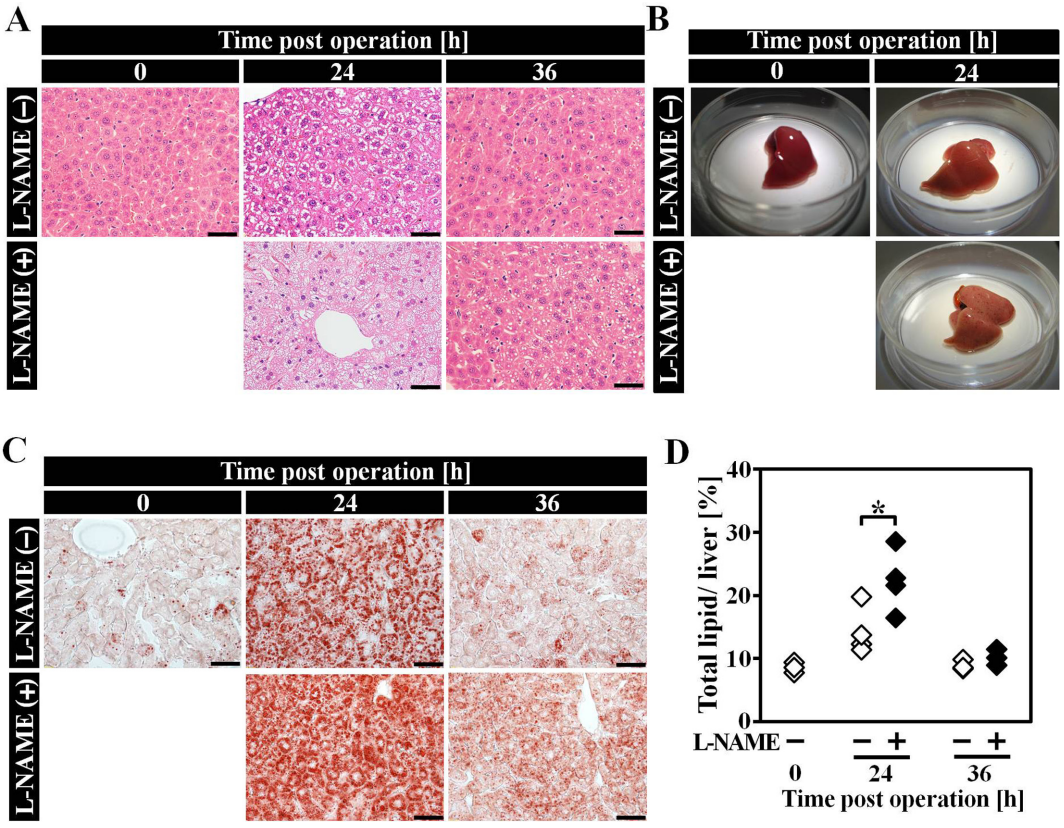

Fig. 2. Hepatic lipid overloading in remnant liver of L-NAME (+) group after hepatectomy. A: HE staining of liver sections at each time point after hepatectomy. B: Liver appearances of PH 0 h and PH 24 h mice. C: ORO staining of liver sections at each time point after hepatectomy. D: Total lipid content in PH remnant liver. n=3–4, the scale bars correspond to 50 μm Data are represented as mean ± SD. * P<0.05.

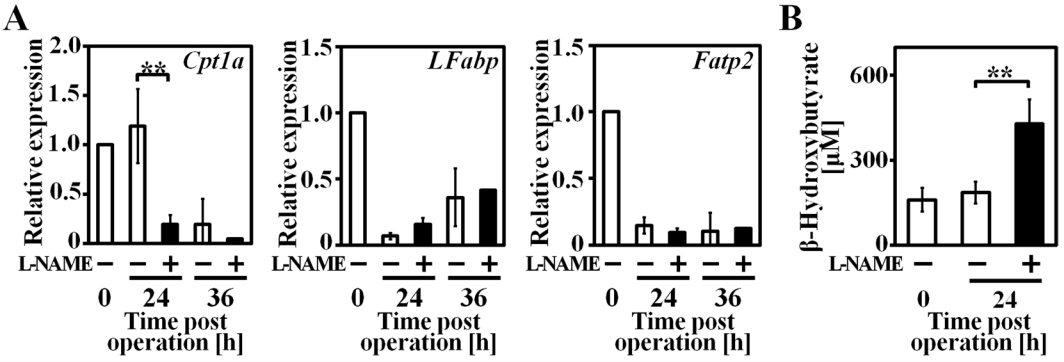

Fig. 3. Expression of genes related to hepatic lipolysis and plasma ketone body concentration were altered in remnant liver of L-NAME (+) group after hepatectomy. A: β-oxidation relative gene expression level. B: Plasma β-hydroxybutyrate concentration. n=3–4, data are represented as mean ± SD. ** P<0.01.

Discussion

By inhibiting all isoforms of NOS, we used this NO depleted mouse model to investigate functions of NO in the regeneration process following PH, revealing its important role to keep hepatic lipolysis activity via IL-6 signaling. Depletion of NO resulted in impaired induction of IL-6 and down-regulation of *Cpt1a*. Because CPT1A functions as the rate-limiting enzyme of fatty acid β-oxidation, down-regulation of *Cpt1a* resulted in

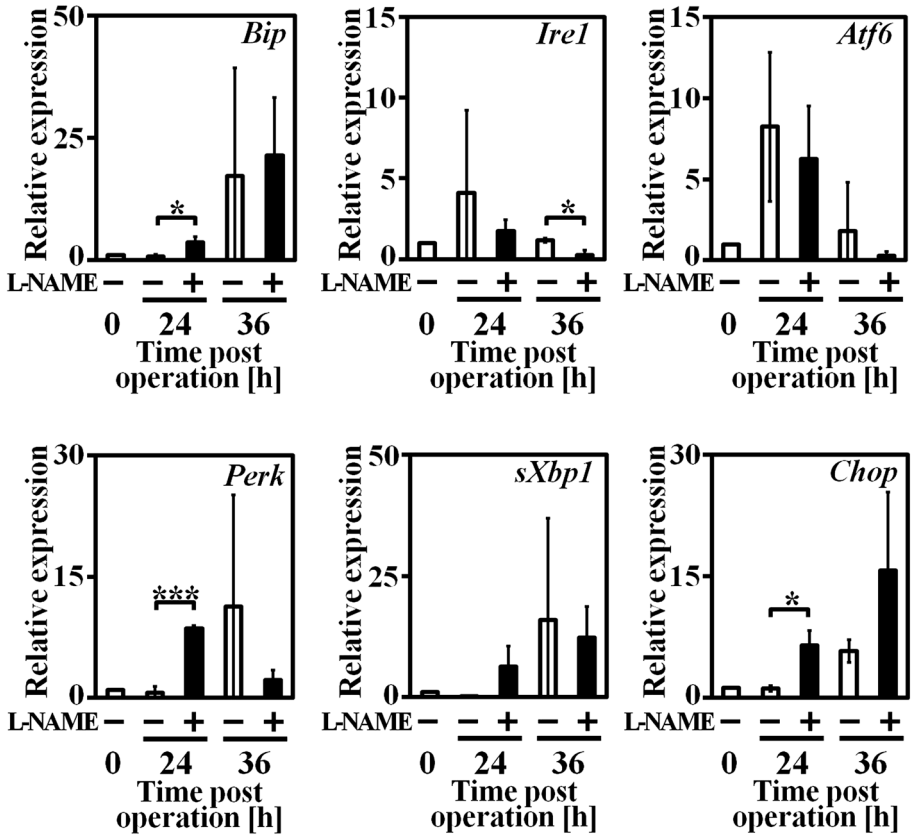

Fig. 4. ER stress relative gene expression in remnant liver tissue at each time point after hepatectomy. n=3–4, data are represented as mean ± SD. * P<0.05, ** P<0.01 and *** P<0.005.

hepatic lipid overloading, elevated ER stress and increased *Chop* expression, consequently impaired hepatocyte proliferation after hepatectomy.

Since NO is an important immune modulator [1, 10, 19] and IL-6 is crucial to trigger mature hepatocyte G0/G1 phase transition through IL-6/gp130/STAT3 pathway [3], Rai *et al.* attempted to investigate whether NO signaling is related to IL-6 expression after hepatectomy [26]. In the isolated macrophage of iNOS KO mouse, *Tnfa* and *IL-6* expression did not decrease as expected, but increased 2–5 folds. However, except Kupffer cell, several types of liver cell could express IL-6 [25, 28, 32], therefore it lacked rationality to study IL-6 expression during liver regeneration by culture of isolated macrophage. In our research, by analyzing activity of IL-6 in peripheral blood of L-NAME administrated mice and WT mice and after hepatectomy, our findings suggested systemic depletion of NO leads to failed induction of IL-6 (Table 2), elucidating the crucial role of NO signaling to induce IL-6 expression after hepatectomy.

Besides the function to prime hepatocyte proliferation in liver regeneration [3], some recent studies have shown that IL-6 also has a function in regulating hepatocyte lipid metabolism [7, 14, 34, 36]. As for different conditions, IL-6 could regulate either lipogenic enzymes expression or lipolytic enzymes expression. For the case of hepatic steatosis, Hong *et al.* reported that long-term subcutaneous administration of IL-6 could ameliorate the symptom of fatty livers, in different animal models as leptin deficient *ob/ob* mice, high fat diet-fed mice, and ethanol-fed mice [15]. In this case, IL-6 treatment stimulated the release of triglyceride and cholesterol from liver into peripheral blood, promoted hepatic fatty acid β-oxidation and increased the expression of peroxisome proliferator-activated receptor α (PPARA) and its DNA binding.

Interestingly, as one of the target genes of PPARA, *Cpt1a* could be up-regulated by IL-6 signaling. After a single treatment with recombinant IL-6 protein to HepG2 cells, *Cpt1a* mRNA level significantly increased [34]. Similar result was observed by porcine adipocytes culture [36]. Moreover, it is reported that CPT1A +/− mice

tended to develop liver steatosis after long-term high-carbohydrate diet or high-fat diet [23], and decreased expression of *Cpt1a* could result in defective mitochondrial fatty acid β-oxidation activity of eNOS KO mice [8]. These results suggest that decreased expression level of CPT1A could affect activity of lipolysis and IL-6 might have a function to promote fatty acid β-oxidation through regulating *Cpt1a* positively. In our result, when IL-6 secretion was severely impaired in L-NAME (+) group after hepatectomy, *Cpt1a* expression decreased significantly compared to L-NAME (−) group (Fig. 3A), and excessive hepatic lipid accumulation was observed (Figs. 2A–D). Average body weight between L-NAME (−) and L-NAME (+) group was not significantly different, excluding the possibility that fasting of L-NAME (+) mice induced excessively accumulated hepatic lipid. However, circulating ketone body β-hydroxybutyrate concentration was higher in L-NAME (+) group mice (Fig. 3B). This could be considered to be a consequence from inactive hepatic energy consumption and higher hepatic TL content in L-NAME (+) group, which is the result of impaired hepatocyte proliferation and NOS inhibition (Fig. 1E).

Rai *et al.* ascribed liver regeneration deficiency of iNOS KO mouse, to the enhanced hepatocyte apoptosis after hepatectomy [26]. Caspase 3 is cleaved to be activated after hepatectomy and NO can inhibit caspase 3 activation by posttranslational regulation [4], thus iNOS deficiency gave rise to more proteolysis in regenerating liver. In our research, we focused on another mechanism between inhibition of NOSs and apoptosis in regenerating liver.

Rodent models with leptin deficiency (*ob/ob* mice) [35], dysfunction of leptin receptor (*fa/fa* rats) [29], or diet-induced NAFLD [11] exhibited deficient liver regeneration after PH, even simple hepatic steatosis induced by high fat diet (HFD) could elevate ER stress and impair liver regeneration ability after hepatectomy [11]. Significantly higher level *Perk* and *Chop* expression were observed in HFD group mice liver than control group. Prolonged ER stress could induce apoptosis through PERK-EIF2A-ATF4 pathway activation and finally induce pro-apoptotic *Chop* expression. As the key mediator of ER stress induced apoptosis, *Chop* could down-regulate the anti-apoptotic gene B-cell lymphoma 2 (*Bcl2*), and up-regulate growth arrest and DNA damage-inducible 34 (*Gadd34*). The duration and intensity of ER stress could control cell fate decisions, from adapting to elevated ER stress, or apoptosis [12, 27]. Our research found hepatic lipid overloading in L-NAME (+) group mice might elevate ER stress in remnant liver (Fig. 4), the over-expression of *Perk* resulted in drastically increased *Chop* expression in PH 24 h and 36 h, revealing the pro-apoptotic pathway was activated.

In summary, our findings suggest the crucial role of NO to liver regeneration in the metabolic perspective. At the first time we found that after hepatectomy, NO depletion could impair IL-6 induction after partial hepatectomy. Together with failed initiation of hepatocyte proliferation, impaired IL-6 expression might also be responsible for down-regulation of *Cpt1a*. Consequently, disturbed fatty acid β-oxidation resulted in hepatic lipid overloading and elevated ER stress. Prolonged ER stress could induce *Chop* expression and activate pro-apoptotic pathway, further impaired hepatocyte proliferation in L-NAME (+) group.

Acknowledgments

This study was supported by a Grant-in-Aid for Scientific Research (A) [No. 25242040] (to YT), for Young Scientists (B) [No. 26750145] (to MT) from the Japan Society for the Promotion of Science (JSPS) and a Grant-in-Aid for Scientific Research on Innovative Areas [No. 231190003] (to YT) from the Ministry of Education, Culture, Sports, Science and Technology of Japan (MEXT) and the Research Program on Hepatitis from Japan Agency for Medical Research and Development (AMED) (to YT).

References

1. Bogdan, C. 2001. Nitric oxide and the immune response. *Nat. Immunol.* 2: 907–916. [Medline] [CrossRef]
2. Bruix, J., Sherman, M., American Association for the Study of Liver Diseases. 2011. Management of hepatocellular carcinoma: an update. *Hepatology* 53: 1020–1022. [Medline] [CrossRef]
3. Cressman, D.E., Greenbaum, L.E., DeAngelis, R.A., Ciliberto, G., Furth, E.E., Poli, V., and Taub, R. 1996. Liver failure and defective hepatocyte regeneration in interleukin-6-deficient mice. *Science* 274: 1379–1383. [Medline] [CrossRef]
4. Dimmeler, S., Haendeler, J., Nehls, M., and Zeiher, A.M. 1997. Suppression of apoptosis by nitric oxide via inhibition of interleukin-1beta-converting enzyme (ICE)-like and cysteine protease protein (CPP)-32-like proteases. *J. Exp. Med.* 185: 601–607. [Medline] [CrossRef]
5. Fausto, N., Campbell, J.S., and Riehle, K.J. 2006. Liver regeneration. *Hepatology* 43:(Suppl 1): S45–S53. [Medline]

[CrossRef]
6. Folch, J., Ascoli, I., Lees, M., Meath, J.A., and LeBARON, N. 1951. Preparation of lipide extracts from brain tissue. *J. Biol. Chem.* 191: 833–841. [Medline]
7. Gavito, A.L., Cabello, R., Suarez, J., Serrano, A., Pavón, F.J., Vida, M., Romero, M., Pardo, V., Bautista, D., Arrabal, S., Decara, J., Cuesta, A.L., Valverde, A.M., Rodríguez de Fonseca, F., and Baixeras, E. 2016. Single administration of recombinant IL-6 restores the gene expression of lipogenic enzymes in liver of fasting IL-6-deficient mice. *Br. J. Pharmacol.* 173: 1070–1084. [Medline] [CrossRef]
8. Le Gouill, E., Jimenez, M., Binnert, C., Jayet, P.Y., Thalmann, S., Nicod, P., Scherrer, U., and Vollenweider, P. 2007. Endothelial nitric oxide synthase (eNOS) knockout mice have defective mitochondrial beta-oxidation. *Diabetes* 56: 2690–2696. [Medline] [CrossRef]
9. Greene, A.K. and Puder, M. 2003. Partial hepatectomy in the mouse: technique and perioperative management. *J. Invest. Surg.* 16: 99–102. [Medline] [CrossRef]
10. Guzik, T.J., Korbut, R., and Adamek-Guzik, T. 2003. Nitric oxide and superoxide in inflammation and immune regulation. *J. Physiol. Pharmacol.* 54: 469–487. [Medline]
11. Hamano, M., Ezaki, H., Kiso, S., Furuta, K., Egawa, M., Kizu, T., Chatani, N., Kamada, Y., Yoshida, Y., and Takehara, T. 2014. Lipid overloading during liver regeneration causes delayed hepatocyte DNA replication by increasing ER stress in mice with simple hepatic steatosis. *J. Gastroenterol.* 49: 305–316. [Medline] [CrossRef]
12. Hetz, C. 2012. The unfolded protein response: controlling cell fate decisions under ER stress and beyond. *Nat. Rev. Mol. Cell Biol.* 13: 89–102. [Medline]
13. Higgins, G.M. and Anderson, R.M. 1931. Experimental pathology of the liver. 1. Restoration of the liver of the white rat following partial surgical removal. *Arch. Pathol.* 12: 186–189.
14. Hong, F., Radaeva, S., Pan, H.N., Tian, Z., Veech, R., and Gao, B. 2004. Interleukin 6 alleviates hepatic steatosis and ischemia/reperfusion injury in mice with fatty liver disease. *Hepatology* 40: 933–941. [Medline] [CrossRef]
15. Huang, J. and Rudnick, D.A. 2014. Elucidating the metabolic regulation of liver regeneration. *Am. J. Pathol.* 184: 309–321. [Medline] [CrossRef]
16. Khedara, A., Goto, T., Morishima, M., Kayashita, J., and Kato, N. 1999. Elevated body fat in rats by the dietary nitric oxide synthase inhibitor, L-N omega nitroarginine. *Biosci. Biotechnol. Biochem.* 63: 698–702. [Medline] [CrossRef]
17. Kopf, M., Baumann, H., Freer, G., Freudenberg, M., Lamers, M., Kishimoto, T., Zinkernagel, R., Bluethmann, H., and Köhler, G. 1994. Impaired immune and acute-phase responses in interleukin-6-deficient mice. *Nature* 368: 339–342. [Medline] [CrossRef]
18. Lirk, P., Hoffmann, G., and Rieder, J. 2002. Inducible nitric oxide synthase--time for reappraisal. *Curr. Drug Targets Inflamm. Allergy* 1: 89–108. [Medline] [CrossRef]
19. MacMicking, J., Xie, Q.W., and Nathan, C. 1997. Nitric oxide and macrophage function. *Annu. Rev. Immunol.* 15: 323–350. [Medline] [CrossRef]
20. Mei, Y. and Thevananther, S. 2011. Endothelial nitric oxide synthase is a key mediator of hepatocyte proliferation in response to partial hepatectomy in mice. *Hepatology* 54: 1777–1789. [Medline] [CrossRef]
21. Merion, R.M. 2010. Current status and future of liver transplantation. *Semin. Liver Dis.* 30: 411–421. [Medline] [CrossRef]
22. Michalopoulos, G.K. and DeFrances, M.C. 1997. Liver regeneration. *Science* 276: 60–66. [Medline] [CrossRef]
23. Nyman, L.R., Tian, L., Hamm, D.A., Schoeb, T.R., Gower, B.A., Nagy, T.R., and Wood, P.A. 2011. Long term effects of high fat or high carbohydrate diets on glucose tolerance in mice with heterozygous carnitine palmitoyltransferase-1a (CPT-1a) deficiency: Diet influences on CPT1a deficient mice. *Nutr. Diabetes* 1: e14. [Medline] [CrossRef]
24. Okazaki, M., Yamada, Y., Nishimoto, N., Yoshizaki, K., and Mihara, M. 2002. Characterization of anti-mouse interleukin-6 receptor antibody. *Immunol. Lett.* 84: 231–240. [Medline] [CrossRef]
25. Panesar, N., Tolman, K., and Mazuski, J.E. 1999. Endotoxin stimulates hepatocyte interleukin-6 production. *J. Surg. Res.* 85: 251–258. [Medline] [CrossRef]
26. Rai, R.M., Lee, F.Y., Rosen, A., Yang, S.Q., Lin, H.Z., Koteish, A., Liew, F.Y., Zaragoza, C., Lowenstein, C., and Diehl, A.M. 1998. Impaired liver regeneration in inducible nitric oxide synthasedeficient mice. *Proc. Natl. Acad. Sci. USA* 95: 13829–13834. [Medline] [CrossRef]
27. Ron, D. and Walter, P. 2007. Signal integration in the endoplasmic reticulum unfolded protein response. *Nat. Rev. Mol. Cell Biol.* 8: 519–529. [Medline] [CrossRef]
28. Saad, B., Frei, K., Scholl, F.A., Fontana, A., and Maier, P. 1995. Hepatocyte-derived interleukin-6 and tumor-necrosis factor alpha mediate the lipopolysaccharide-induced acute-phase response and nitric oxide release by cultured rat hepatocytes. *Eur. J. Biochem.* 229: 349–355. [Medline] [CrossRef]
29. Selzner, M. and Clavien, P.A. 2000. Failure of regeneration of the steatotic rat liver: disruption at two different levels in the regeneration pathway. *Hepatology* 31: 35–42. [Medline] [CrossRef]
30. Tagawa, Y., Matthys, P., Heremans, H., Dillen, C., Zaman, Z., Iwakura, Y., and Billiau, A. 2000. Bimodal role of endogenous interleukin-6 in concanavalin A-induced hepatitis in mice. *J. Leukoc. Biol.* 67: 90–96. [Medline]
31. Tamai, M., Yamashita, A., and Tagawa, Y. 2011. Mitochondrial development of the in vitro hepatic organogenesis model with simultaneous cardiac mesoderm differentiation from murine induced pluripotent stem cells. *J. Biosci. Bioeng.* 112: 495–500. [Medline] [CrossRef]
32. Thirunavukkarasu, C., Watkins, S.C., and Gandhi, C.R. 2006. Mechanisms of endotoxin-induced NO, IL-6, and TNF-alpha production in activated rat hepatic stellate cells: role of p38 MAPK. *Hepatology* 44: 389–398. [Medline] [CrossRef]
33. Tralhão, J.G., Abrantes, A.M., Hoti, E., Oliveiros, B., Cardoso, D., Faitot, F., Carvalho, C., Botelho, M.F., and Castro-Sousa, F. 2014. Hepatectomy and liver regeneration: from experimental research to clinical application. *ANZ J. Surg.* 84: 665–671. [Medline] [CrossRef]

34. Vida, M., Serrano, A., Romero-Cuevas, M., Pavón, F.J., González-Rodriguez, A., Gavito, A.L., Cuesta, A.L., Valverde, A.M., Rodríguez de Fonseca, F., and Baixeras, E. 2013. IL-6 cooperates with peroxisome proliferator-activated receptor-α-ligands to induce liver fatty acid binding protein (LFABP) up-regulation. *Liver Int.* 33: 1019–1028. [Medline] [CrossRef]
35. Yang, S.Q., Lin, H.Z., Mandal, A.K., Huang, J., and Diehl, A.M. 2001. Disrupted signaling and inhibited regeneration in obese mice with fatty livers: implications for nonalcoholic fatty liver disease pathophysiology. *Hepatology* 34: 694–706. [Medline] [CrossRef]
36. Yang, Y., Ju, D., Zhang, M., and Yang, G. 2008. Interleukin-6 stimulates lipolysis in porcine adipocytes. *Endocrine* 33: 261–269. [Medline] [CrossRef]
37. Zhao, Y., Vanhoutte, P.M., and Leung, S.W.S. 2015. Vascular nitric oxide: Beyond eNOS. *J. Pharmacol. Sci.* 129: 83–94. [Medline] [CrossRef]
38. Zhou, L. and Zhu, D.Y. 2009. Neuronal nitric oxide synthase: structure, subcellular localization, regulation, and clinical implications. *Nitric Oxide* 20: 223–230. [Medline] [CrossRef]